

A Numerical Study on Soot Formation and Evolution in Pressurized Turbulent Sooting Flames

Dezhi Zhou*, Anders Vaage[†], Suo Yang[‡]

Department of Mechanical Engineering, University of Minnesota – Twin Cities, Minneapolis, MN 55455, USA

Wesley Boyette[§], Thibault Guiberti[¶], William Roberts[∥] *Mechanical Engineering, King Abdullah University of Science and Technology, Thuwal 23955, Saudi Arabia*

Understandings on soot formation and evolution in pressurized flames are of significant interest due to the increasing operating pressures in different combustors and the accompanying increased soot emissions. In this study, a series of pressurized turbulent sooting flames at 1 bar, 3 bar and 5 bar, are simulated to study the pressure effect on the soot formation and evolution. The inflow conditions are chosen such that the Reynolds number at different pressures keep constant. Via a Radiation Flamelet Progress Variable (RFPV) approach with a conditional soot sub-filter Probability Density Function (PDF) to consider the turbulence-chemistry-soot interaction, quantitatively good agreements (e.g., maximum discrepancy within one order of magnitude) are achieved for soot volume fraction predictions compared with the experimental data at different pressures. Soot volume fraction source terms are then discussed to show the pressure effect on nucleaion, condensation, surface growth and oxidation at different axial positions in these flames.

I. Introduction

To achieve higher efficiency, combustion is nowadays pushed to extremely high pressure limits, such as the supercritical combustion in sCO2 combustors and high-pressure combustion in pressure gain engines. As such, it is fundamentally needed to understand the pressure effect on combustion. There exists a few computational works investigating the pressure effect on turbulent non-premixed flames. Tabet et al. [II] studied turbulent non-premixed hydrogen-air flame structure in pressure range of 1-10 atm, in which, the pressure is found to increase the gas density and thus change the flame structure. Other studies such as Hong et al. [2] studied the pressure effect on a non-premixed turbulent flame, reporting a more focused flame with high pressures. Under high pressures conditions, one major concern is the dramatically increased soot emissions, as experimentally observed in many pressurized laminar and turbulent sooting flames [3]-[6]. Soot is the major pollutants in the air, as the form of particulate matter. In addition, soot is also the major agent responsible for climate change. It is hence vital to understand the mechanisms of soot formation and evolution in high pressure combustion.

To understand the pressure effect on soot formation and evolution, many numerical studies on pressurized laminar flames have been conducted to show that the change of polycyclic aromatic hydrocarbons (PAH) concentration, scalar dissipation rate, and the different chemical pathways are the major issues for the increasing soot at higher pressures [7]. 8]. However, there lack studies on the soot formation and evolution in pressurized turbulent flames due to two reasons. First of all, it is well recognized that developing predictive models for turbulent sooting flames is very challenging due to the complicated interactions among turbulence, detailed chemistry and soot. Secondly, measurements of key parameters such as temperature and major species in turbulent flames is significant for the comparison and validation of computational models. Although there are a variety of measurement of soot quantities in atmospheric turbulent sooting flames, the measurement of these parameters are not easy for pressurized flames, due to the high soot volume fraction under elevated pressures and thus the interfered combustion zone. The successful measurement in a swirl gas turbine model combustor (DLR) with elevated pressures, to the best knowledge of the authors, is the only available data

^{*}Post-Doctoral Associate, Member AIAA.

[†]Undergraduate Student.

[‡]Richard & Barbara Nelson Assistant Professor, suo-yang@umn.edu (Corresponding Author), Member AIAA.

[§]Post-Doctoral Associate, Member AIAA.

Research Scientist, Member AIAA.

Professor and Director of Clean Combustion Research Center, Senior Member AIAA

for pressurized turbulent sooting flame data [6]. The computational study in Chong *et al.* [9] studied the pressure and dilution-jet effect on soot formation in this aircraft swirl combustor. However, it is seen that in this numerical study the soot prediction has over one order of magnitude error when comparing with experimental data at high pressures. It is reported in this study that the discrepancy is due to the chemical/physical models uncertainty, which however, is not discussed in detail. To obtain more fundamental understanding on the pressure effect on soot formation and evolution in pressurized turbulent sooting flames, a simpler and well-understood configuration without too complex geometry and flow (e.g., turbulent jet flames) is needed.

Recently, Boyette *et al.* [10] established a high-pressure turbulent sooting flame configuration (KEN flames) by diluting the fuel with N2, allowing a non-sooting region for temperature and major species measurements. In this study, we for the first time simulated the KEN turbulent jet sooting flames with the pressure ranges from 1 -5 bar. A recently proposed conditional soot sub-filter probability density function (PDF) [11] is used in this study to account for the turbulence-soot-chemistry interaction. Under different pressures, prediction accuracy within one order of magnitude is achieved. Pressure effect on soot formation and evolution is then analyzed and discussed in this study.

II. Methodology

A. Turbulent combustion modeling

In this study, the Radiation Flamelet/Progress Variable (RFPV) [12] [13] is used to decouple the detailed flame structure from the computation of flow field. The non-premixed flame structure *a priori* computed in the mixture fraction space, forming a series of steady non-premixed flamelet solutions with different radiation heat losses and mixture fraction dissipation rates. Radiation is modeled with an optically thin gray gas approach, where the absorption coefficients for CO₂, H₂O, CH₄, and CO are obtained from Barlow *et al.* [14]. The KM2 chemical reaction model [15] is used in this study when computing the non-premixed flamelet solutions.

B. Soot modeling

A bivariate parameteraization (volume and surface area) of the Number Density Function (NDF) is employed to model detailed aggregation of soot. To avoid the computationally expensive solution of every soot number density function and yet capture the global quantities of soot formation and evolution, the method of moments (MOM) is used. In MOM, the joint moments of the NDF are given by

$$M_{x,y} = \sum_{i=0}^{\infty} V_i^x S_i^y N_i, \tag{1}$$

where summation over i implies summation over the entire two-dimensional state space and N_i is then the number density of particles of volume V_i and surface area S_i . The subscripts x and y denote the order of the moment in volume and surface area, respectively. In this study, four moments are transported while their source terms are closed with the Hybrid Method of Moments (HMOM) [16].

C. Transport equations

In this study, large eddy simulations (LES) are used, which apply filtering operations to the conservation equations for momentum and scalars. More specifically, the filtered transport equations are given by

$$\frac{\partial \bar{\rho} \widetilde{Z}}{\partial t} + \frac{\partial \bar{\rho} \widetilde{u}_i \widetilde{Z}}{\partial x_i} = \frac{\partial}{\partial x_i} \left(\bar{\rho} \widetilde{u}_i \widetilde{Z} - \bar{\rho} \widetilde{u}_i \widetilde{Z} \right) + \frac{\partial}{\partial x_i} \left(\bar{\rho} \widetilde{D}_Z \frac{\partial \widetilde{Z}}{\partial x_i} \right) + \overline{\dot{m}}_Z, \tag{2}$$

$$\frac{\partial \bar{\rho} \widetilde{C}}{\partial t} + \frac{\partial \bar{\rho} \widetilde{u}_i \widetilde{C}}{\partial x_i} = \frac{\partial}{\partial x_i} \left(\bar{\rho} \widetilde{u}_i \widetilde{C} - \bar{\rho} \widetilde{u}_i \widetilde{C} \right) + \frac{\partial}{\partial x_i} \left(\bar{\rho} \widetilde{D}_C \frac{\partial \widetilde{C}}{\partial x_i} \right) + \overline{\dot{m}}_C, \tag{3}$$

$$\frac{\partial \bar{\rho} \widetilde{H}}{\partial t} + \frac{\partial \bar{\rho} \widetilde{u}_i \widetilde{H}}{\partial x_i} = \frac{\partial}{\partial x_i} \left(\bar{\rho} \widetilde{u}_i \widetilde{H} - \bar{\rho} \widetilde{u}_i \widetilde{H} \right) + \frac{\partial}{\partial x_i} \left(\bar{\rho} \widetilde{D}_H \frac{\partial \widetilde{H}}{\partial x_i} \right) + \overline{\dot{\rho}} \overline{H} + \overline{\dot{q}}_{RAD}, \tag{4}$$

$$\frac{\partial \bar{\rho} \widetilde{Y}_{\mathrm{PAH}}}{\partial t} + \frac{\partial \bar{\rho} \widetilde{u}_{i} \widetilde{Y}_{\mathrm{PAH}}}{\partial x_{i}} = \frac{\partial}{\partial x_{i}} \left(\bar{\rho} \widetilde{u}_{i} \widetilde{Y}_{\mathrm{PAH}} - \bar{\rho} \widetilde{u_{i} Y_{\mathrm{PAH}}} \right) + \frac{\partial}{\partial x_{i}} \left(\bar{\rho} \widetilde{D}_{\mathrm{PAH}} \frac{\partial \widetilde{Y}_{\mathrm{PAH}}}{\partial x_{i}} \right) + \overline{\dot{m}}_{\mathrm{PAH}},$$

$$\frac{\partial \overline{M}_{j}}{\partial t} + \frac{\partial \widetilde{u_{i}^{*}} \overline{M}_{j}}{\partial x_{i}} = \frac{\partial}{\partial x_{i}} \left(\widetilde{u_{i}^{*}} \overline{M}_{j} - \overline{u_{i}^{*}} \overline{M}_{j} \right) + \overline{\dot{M}}_{j}, \tag{5}$$

where the overline indicates the filtering operation, and the tilde implies a density-weighted filtering. For each equation, the first term on the right-hand side is known as the subfilter scalar flux and contains the effects of unresolved turbulent transport; the second term is the filtered molecular diffusion fluxes (except for the soot moment equations). The models to close those terms are well-established in the literature and thus not discussed here in detail. The last term in these equations is the filtered source term, including the filtered reaction source term and moments source term, which are discussed in the following section.

D. Turbulence-chemistry-soot interaction

To model the subfilter soot-turbulence-chemistry interactions, the filtered source term $\overline{\dot{Q}}$ is usually closed through convolution with a density-weighted joint subfilter PDF $\widetilde{P}(\xi_i, M_j)$, which is a function of the vector of thermochemical variables ξ_i and the vector of soot variables M_j .

$$\overline{\dot{Q}}\left(\widetilde{\xi_i}, \overline{M}_j\right) = \iint \dot{Q}(\xi_i, M_j) \widetilde{P}(\xi_i, M_j) d\xi_i dM_j. \tag{6}$$

The joint subfilter PDF $\widetilde{P}(\xi_i, M_j)$ is unknown and must be modeled using transported PDF or presumed PDF approaches. The presumed PDF approach will be adopted in this work. Following the recently proposed method in $[\Pi]$. The soot-chemistry-turbulence interaction is considered by a conditional soot sub-filter PDF, which only activates the sooting mode at fuel-rich mixture fractions when oxidation is slower than surface growth.

E. Experimental and numerical configuration

KEN flames are turbulent piloted jet flames. The fuel jet is composed of ethylene diluted with 65% (by volume) nitrogen. The fuel central inner inlet diameter is D=3.4 mm. The flame is stablized by a pilot providing 18% of the heat release of the jet. The piloted flames are pre-mixtures of C_2H_4 /air with equivalence ratio 0.9. The surrounding co-flow is air and the co-flow diameter is 19.05 mm. The jet velocity (U_j) , air co-flow velocity (U_c) and Reynolds number (Re) of the simulated cases are listed in Table [I]

Table 1 Operating conditions of the simulated cases, following the experimental details in [10].

Case	Pressure (bar)	Re	U_j (m/s)	U_c (m/s)
1	1	10000	36.6	0.6
2	3	10000	12.2	0.2
3	5	10000	7.32	0.12

To simulate KEN flames with LES, a cylindrical computational domain with 300D in the axial direction is discretized into $192 \times 96 \times 32$ in the axial, radial and azimuthal direction, respectively. The grid points are concentrated near the

mixing and combustion regions by stretching the grid in the downstream direction axially and keeping uniform spaced grid in the circumferential direction, with 0.1 mm as the minimum grid size. To account for the turbulent inlet velocity profile, a separate periodic pipe flow simulation is firstly conducted with the mean axial velocity values as indicated in Table and then enforced as the boundary conditions for the turbulent flame simulations. The simulations are run over 10 flow through time to reach statistically stationary status and then another over 10 flow through time is run to collect statistics.

III. Results and Discussion

A. Soot volume fraction

We firstly compared our predicted soot volume fraction with the experimental data to show the good accuracy of our numerical models and framework. Figure shows the comparison of the predicted (time avaeraged) and measured soot volume fraction at the flame centerline. As seen for all the three pressures, the predicted time averaged soot volume fractions capture the measured data very well (i.e., the discrepancy is within one order of magnitude). More specifically, our model underpredicts 4 times at 1 bar, while overpredicts 4 times at 5 bar.

To further validate the predictability of our numerical framework, the soot volume fractions at different axial positions are shown in Fig. 2 3 and 4 to compare the predicted and measured quantities. Again, very good agreements are achieved at 6 different axial positions, at 1, 3 and 5 bar. More specifically, it is seen that at 1 bar, the simulations underpredict soot volume fraction by 6 times. At 3 bar, the predicted soot region is generally narrower than the experimental data while the soot volume fractions are captured very well. At 5 bar, the simulation over predict the soot volume fraction by 5 times. A four times difference is observed, which is considered to be accurate, compared with other simulation result for the same case 17 (a more than 10 times difference). The discrepancy at different pressure is consistent with the observation at the centerline results (i.e., Fig. 1). With the increasing pressure, although the prediction is very accurate, the model tends to predict more soot foramtions. This indicates that our numerical model is correlated with pressure (i.e., pressure dependent), which merits future study to further improve the model prediction at various pressures.

B. Soot volume fraction source terms

The soot volume fraction source terms, including nucleation, condensation, surface growth and oxidation are discussed at three different axial positions in this section, for all the three pressures. These soot volume fraction source terms are plotted in the mixture fraction space. As seen in Fig. 5 the increasing pressure significantly increase the rate of nucleation and condensation, which may be attributed to the higher PAH precursor concentration at elevated pressures. It is also noted that the increasing pressure pushes the nucleation and condensation to less rich regions. In addition, at x = 0.234 where there are large soot volume fractions for all the three pressures, condensation is dominant over nucleation due to the large values of existing soot volume fractions at this position. At more downstream (x = 0.314), nucleation is then stronger than condensation due to the almost oxidized soot at this position. The normalized surface growth and oxidation rates in the mixture fraction space are shown in Fig. 6. As seen, the normalized surface growth and oxidation rates are not enhanced by the increasing pressure, suggesting that the major reason for increased surface growth and oxidation are due to the increased soot volume fraction and thus the increased surface area of soot particles.

IV. Conclusions and Future Work

In this study, detailed simulations for turbulent sooting flames at elevated pressures are conducted to analyze the soot formation and evolution at elevated pressures. A conditional soot sub-filter PDF method with RFPV and HMOM are used for turbulent combustion and soot modeling. A series of KEN flames at 1, 3 and 5 bar are studied. Our numerical framework with RFPV as the turbulent combustion mdoel, HMOM for the soot modeling, and a conditional soot subfilter PDF for the turbulence-chemistry-soot interaction, predict the soot volume fraction at different positions for all the three pressures with very good accuracy (maximum discrepancy within one order of magnitude). In addition, the soot volume fraction source terms, including nucleation, condensation, surface growth and oxidation terms, are discussed and analyzed. It is observed that the increasing pressure could significantly increase the nucleation and condensation rate. For all the three pressures, condensation is dominant over nucleation at the position where soot volume fraction peaks. In addition, it is seen that in these turbulent jet sooting flames, the normalized surface growth and oxidation are not enhanced by the increasing pressure. For future work, we plan to further analyze the chemistry

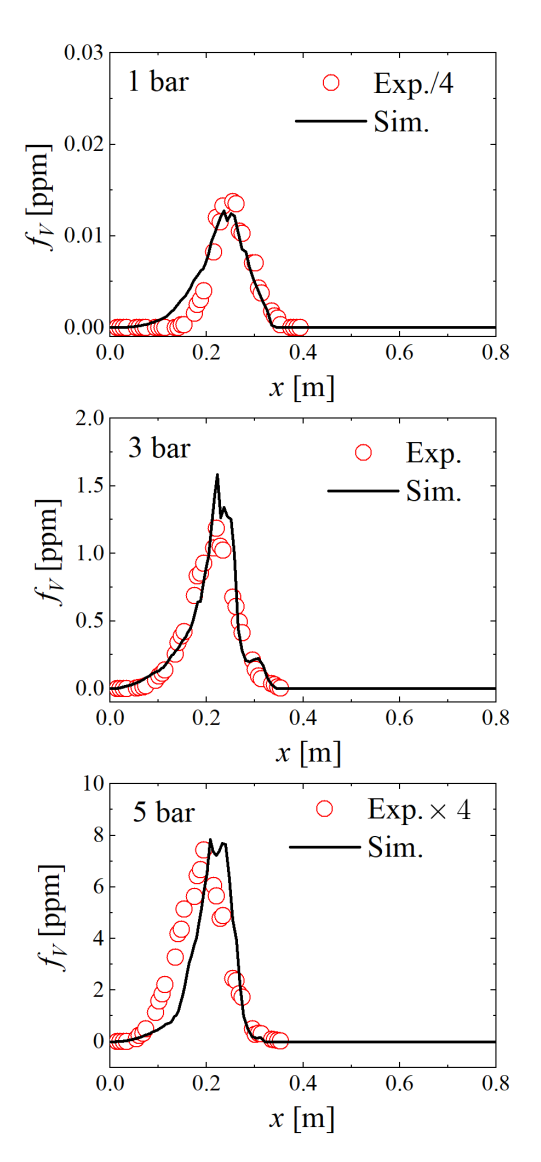


Fig. 1 Predicted and measured soot volume fractions (f_V) , as a function of the axial distance (x) in the centerline.

uncertainty under high pressure in turbulent sooting flames. To conduct chemistry flux analysis for soot formation, our newly proposed method (i.e., soot-based global pathway analysis) will be used to identify the controlling reaction pathway way for soot formation and evolution.

Acknowledgments

S. Yang gratefully acknowledges the faculty start-up funding from the University of Minnesota and the grant support from NSF CBET 2038173. Part of the simulation was conducted on the computational resources from the Minnesota Supercomputing Institute (MSI).

References

- [1] Tabet, F., Sarh, B., and Gökalp, I., "Turbulent non-premixed hydrogen-air flame structure in the pressure range of 1–10 atm," *international journal of hydrogen energy*, Vol. 36, No. 24, 2011, pp. 15838–15850.
- [2] Hong, S., Lee, W., Kang, S., and Song, H. H., "Analysis of turbulent diffusion flames with a hybrid fuel of methane and

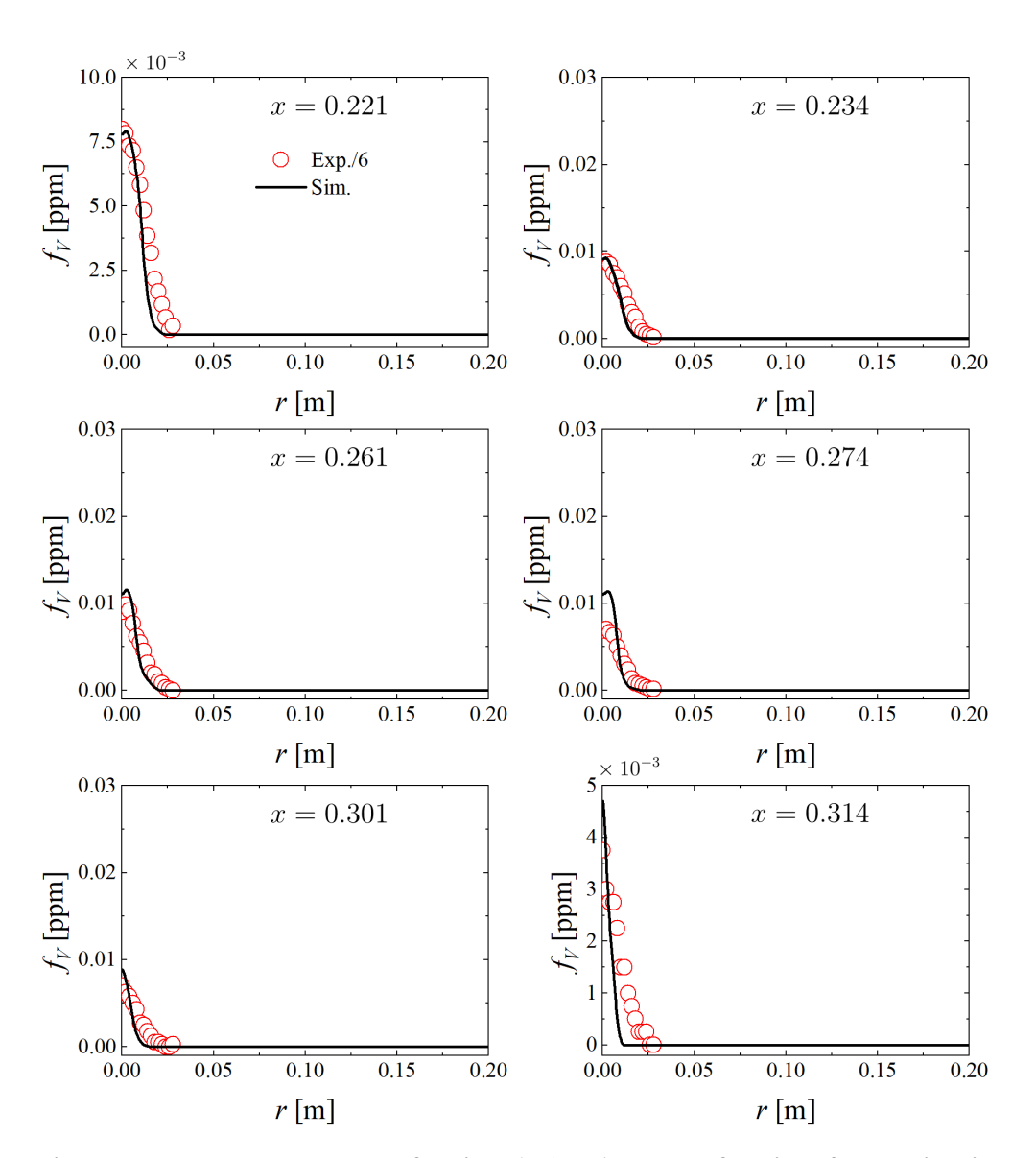


Fig. 2 Predicted and measured soot volume fractions (f_V) at 1 bar, as a function of the radial distance (r) at different axial positions.

hydrogen in high pressure and temperature conditions using LES approach," *International Journal of Hydrogen Energy*, Vol. 40, No. 35, 2015, pp. 12034–12046.

- [3] Kailasanathan, R. K. A., Yelverton, T. L., Fang, T., and Roberts, W. L., "Effect of diluents on soot precursor formation and temperature in ethylene laminar diffusion flames," *Combust. Flame*, Vol. 160, No. 3, 2013, pp. 656–670.
- [4] Kailasanathan, R. K. A., Book, E. K., Fang, T., and Roberts, W. L., "Hydrocarbon species concentrations in nitrogen diluted ethylene-air laminar jet diffusion flames at elevated pressures," *Proc. Combust. Inst.*, Vol. 34, No. 1, 2013, pp. 1035–1043.
- [5] Steinmetz, S. A., Fang, T., and Roberts, W. L., "Soot particle size measurements in ethylene diffusion flames at elevated pressures," *Combust. Flame*, Vol. 169, 2016, pp. 85–93.
- [6] Geigle, K. P., Köhler, M., O'Loughlin, W., and Meier, W., "Investigation of soot formation in pressurized swirl flames by laser measurements of temperature, flame structures and soot concentrations," *Proceedings of the Combustion Institute*, Vol. 35, No. 3, 2015, pp. 3373–3380.

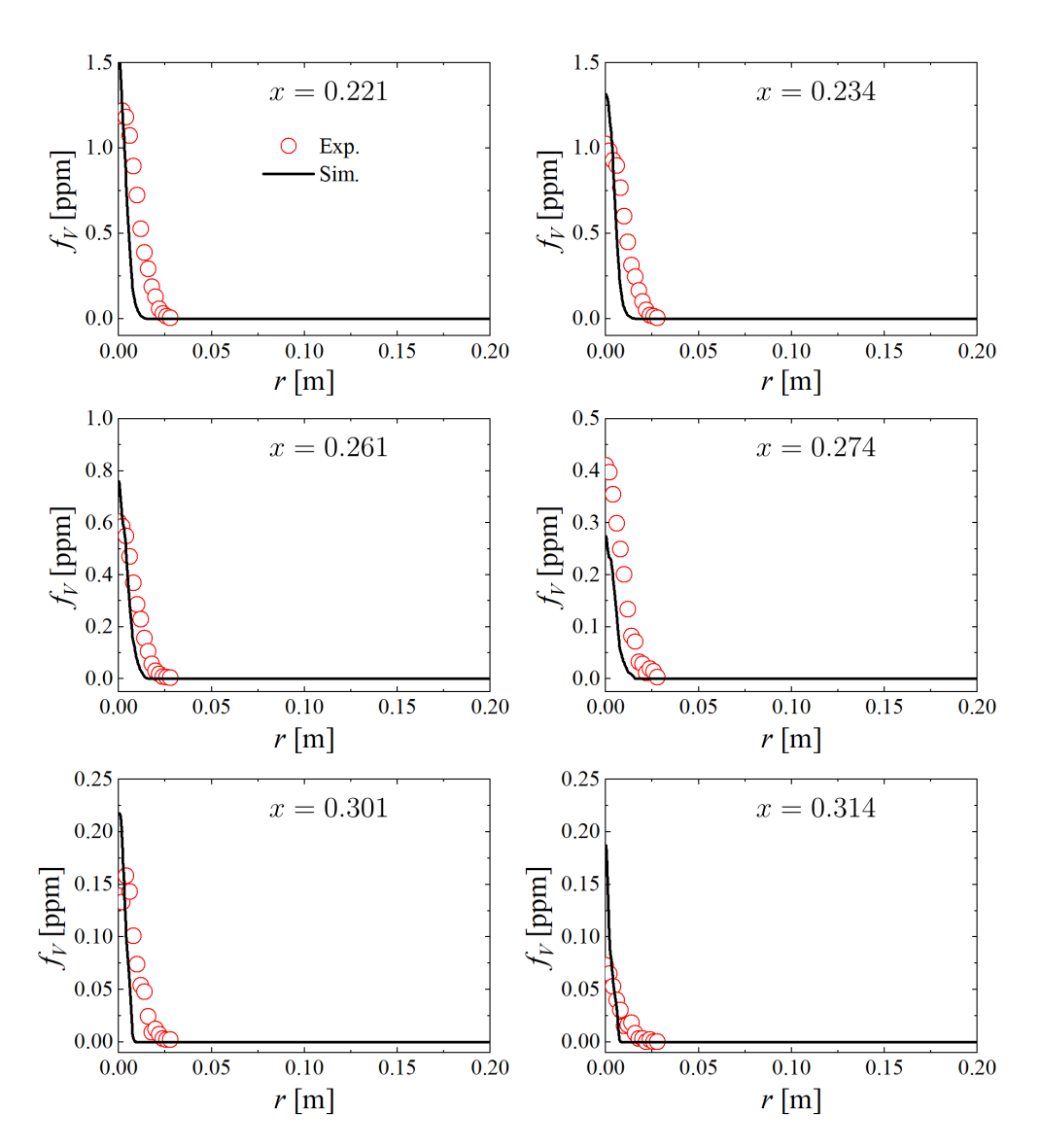


Fig. 3 Predicted and measured soot volume fractions (f_V) at 3 bar, as a function of the radial distance (r) at different axial positions.

- [7] Abdelgadir, A., Rakha, I. A., Steinmetz, S. A., Attili, A., Bisetti, F., and Roberts, W. L., "Effects of hydrodynamics and mixing on soot formation and growth in laminar coflow diffusion flames at elevated pressures," *Combust. Flame*, Vol. 181, 2017, pp. 39–53.
- [8] Zhou, D., Zou, S., and Yang, S., "A Numerical Study on Soot Formation and Evolution in Co-flow Diffusion Flames under Elevated Pressures," *AIAA Scitech 2020 Forum*, 2020, p. 1658.
- [9] Chong, S. T., Hassanaly, M., Koo, H., Mueller, M. E., Raman, V., and Geigle, K.-P., "Large eddy simulation of pressure and dilution-jet effects on soot formation in a model aircraft swirl combustor," *Combustion and Flame*, Vol. 192, 2018, pp. 452–472.
- [10] Boyette, W. R., Elbaz, A. M., Guiberti, T. F., and Roberts, W. L., "Experimental investigation of the near field in sooting turbulent nonpremixed flames at elevated pressures," *Experimental Thermal and Fluid Science*, Vol. 105, 2019, pp. 332–341.
- [11] Yang, S., Lew, J. K., and Mueller, M. E., "Large Eddy Simulation of soot evolution in turbulent reacting flows: Presumed subfilter PDF model for soot–turbulence–chemistry interactions," *Combustion and Flame*, Vol. 209, 2019, pp. 200–213.
- [12] Ihme, M., and Pitsch, H., "Modeling of radiation and nitric oxide formation in turbulent nonpremixed flames using a flamelet/progress variable formulation," *Physics of Fluids*, Vol. 20, No. 5, 2008, p. 055110.

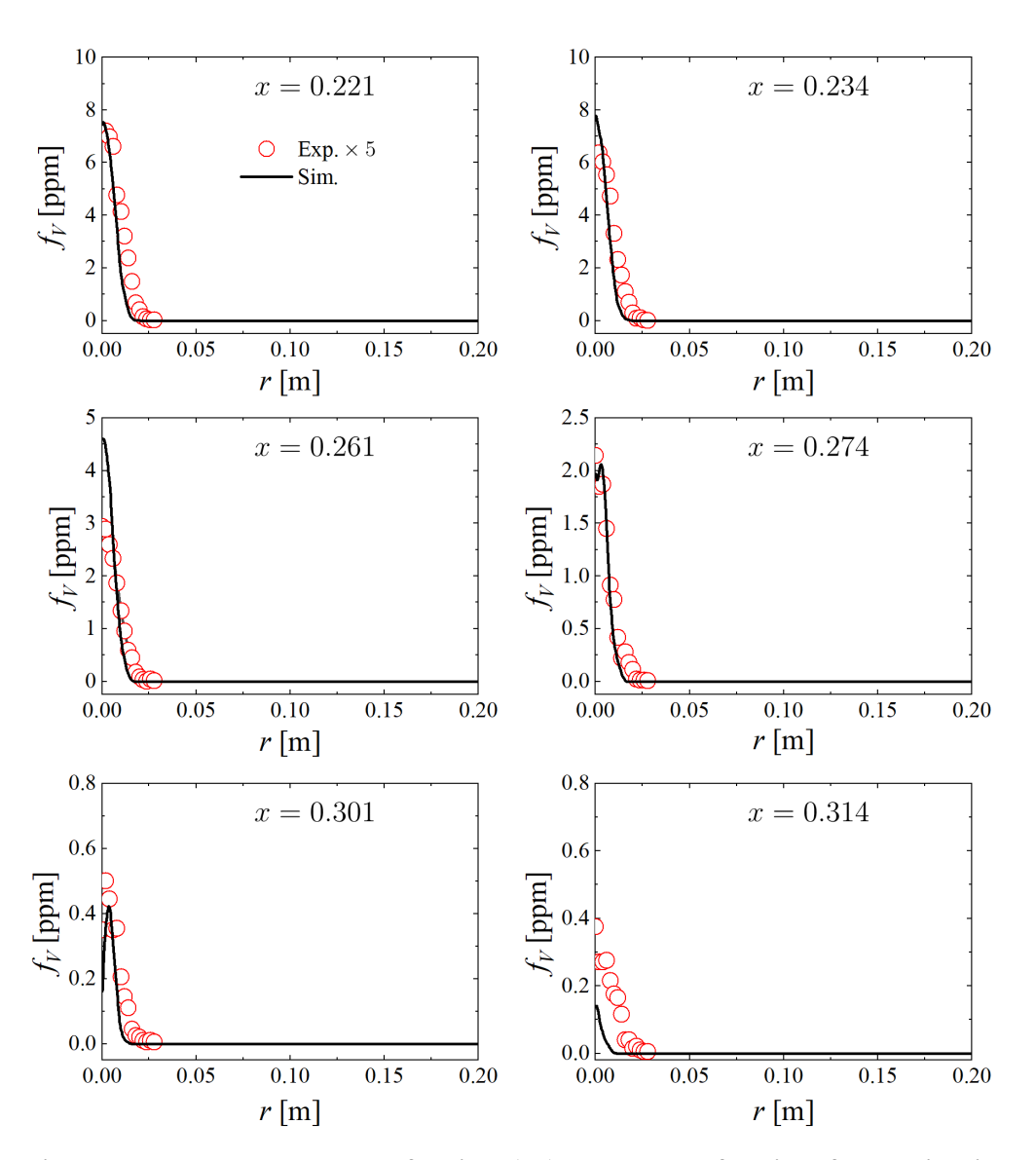


Fig. 4 Predicted and measured soot volume fractions (f_V) at 5 bar, as a function of the radial distance (r) at different axial positions.

- [13] Mueller, M. E., and Pitsch, H., "LES model for sooting turbulent nonpremixed flames," *Combustion and Flame*, Vol. 159, No. 6, 2012, pp. 2166–2180.
- [14] Barlow, R. S., Karpetis, A. N., Frank, J. H., and Chen, J.-Y., "Scalar profiles and NO formation in laminar opposed-flow partially premixed methane/air flames," *Combust. Flame*, Vol. 127, No. 3, 2001, pp. 2102–2118. doi:10.1016/S0010-2180(01)00313-3.
- [15] Wang, Y., Raj, A., and Chung, S. H., "A PAH growth mechanism and synergistic effect on PAH formation in counterflow diffusion flames," *Combustion and flame*, Vol. 160, No. 9, 2013, pp. 1667–1676.
- [16] Mueller, M. E., Blanquart, G., and Pitsch, H., "Hybrid method of moments for modeling soot formation and growth," *Combustion and Flame*, Vol. 156, No. 6, 2009, pp. 1143–1155.
- [17] Schiener, M., and Lindstedt, R., "Transported probability density function based modelling of soot particle size distributions in non-premixed turbulent jet flames," *Proceedings of the Combustion Institute*, Vol. 37, No. 1, 2019, pp. 1049–1056.

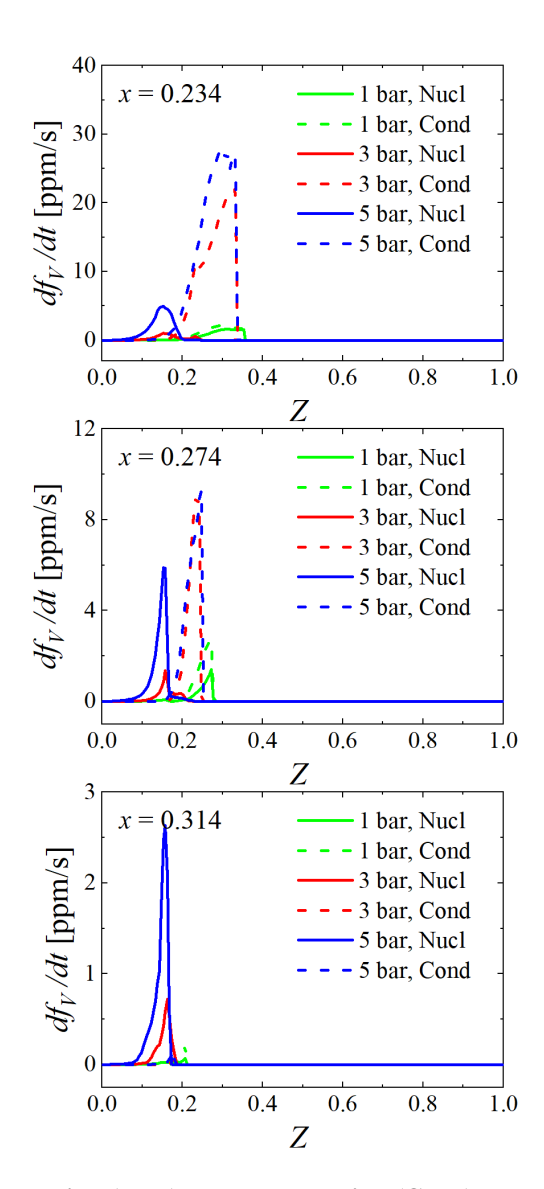


Fig. 5 Soot volume fraction nucleation (Nucl) and condensation (Cond) source terms in the mixture fraction space.

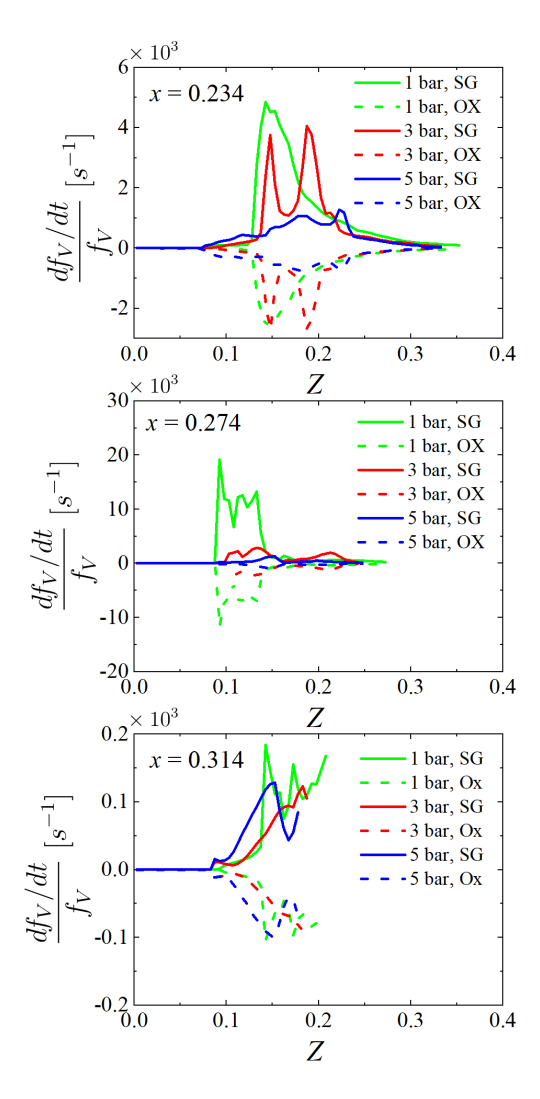


Fig. 6 Normalized soot volume fraction surface growth (SG) and oxidation (OX) source terms in the mixture fraction space.